

# **AN ENHANCED, CONSTANT ENVELOPE, INTEROPERABLE SHAPED OFFSET QPSK (SOQPSK) WAVEFORM FOR IMPROVED SPECTRAL EFFICIENCY**

**Terrance J. Hill**  
Nova Engineering, Inc., Cincinnati, OH

## **ABSTRACT**

Shaped BPSK (SBPSK) and Shaped Offset QPSK (SOQPSK), as defined in various MIL standards, are widely employed on SATCOM links because they offer an attractive combination of good spectral efficiency, constant envelope characteristics, and interoperability with legacy equipments. More recently, numerous terrestrial applications of OQPSK and similar waveforms (Feher-patented FQPSK) have been proposed. The present paper describes a simple non-proprietary modification of the MIL-STD SOQPSK waveform which offers spectral containment and detection efficiency comparable to or better than FQPSK-B (Revision A1), while preserving a constant envelope characteristic and backward compatibility with existing equipment.

## **KEY WORDS**

Shaped Offset QPSK, FQPSK, Spectral Occupancy, Constant Envelope, Bandwidth Efficiency

## **INTRODUCTION**

Shaped BPSK (SBPSK) was introduced in the early 1980's (MILCOM '84, SBPSK: A Robust Bandwidth-Efficient Modulation for Hard-Limited Channels) as a means of bandlimiting a BPSK signal, while keeping the signal envelope constant. The advantage to maintaining a constant envelope is that the spectral sidelobes do not regenerate when the signal is passed through a limiting, or otherwise nonlinear, amplifier. The first implementation of SBPSK was in the AN/PSC-1, operating in the 225 – 400 MHz SATCOM band. The waveform's high degree of success in that role led eventually to its adoption as a standard for the UHF SATCOM terminals as described in MIL-STD-188-181, and 188-182. Further development of the SBPSK concept led to an Offset QPSK variant called, naturally enough, SOQPSK, which is also defined in the same MIL-STDs.

In this paper, we will briefly review the MIL-STD SOQPSK waveform, introduce two new frequency shaping pulses which improve spectral containment, and then compare the BER performance and spectral efficiency to other OQPSK variants, including Feher-patented FQPSK-B (Revision A1).

## OQPSK AS FREQUENCY MODULATION

Offset QPSK can be viewed as either a phase modulation or a frequency modulation. Because the shaped variants of OQPSK are best interpreted from a frequency modulation viewpoint, we will adopt the FM description here. If we use the notation commonly employed for Continuous Phase Modulation (CPM) waveforms, OQPSK is defined by

$$s(t) = \sqrt{2E/(T/2)} \cos[2\pi f_c t + \phi(t, \bar{\alpha}) + \phi_o] \text{ where}$$

$$\phi(t, \bar{\alpha}) = 2\pi h \int_{-\infty}^t \sum_{i=-\infty}^{+\infty} \alpha_i g(\tau - iT/2) d\tau \quad -\infty < t < +\infty$$

The information-bearing phase  $\phi(t, \bar{\alpha})$  is determined by the 3-ary sequence  $\alpha_i = -1, 0, 1$ , the unity-area frequency pulse  $g(t)$ , and the modulation index  $h$ , which is equal to  $1/4$  for offset QPSK. The 3-state values for  $\alpha_i$  stem from the offset between the I and Q channels, which constrains the phase to either advance or retard by  $\pi/2$  radians, or not change at all. Note that  $T$  in these expressions is the symbol period, not the bit period.

For unshaped OQPSK, the frequency pulse  $g(t)$  is simply a unit-area delta function,  $\delta(t)$ . In each bit period the frequency pulse is either present or absent. If present, the phase will shift by  $\pi/2$  radians, but it can only go in the “allowed” direction for that bit period. Because of the offset between the I and Q channels, the allowed direction will depend on the current state, such that the signal will change in I value, or Q, but never both at the same time. The top trace in Figure 1 depicts the unshaped case.

The MIL-STD version of SOQPSK is depicted by the middle trace in Figure 1. Again, the area of the frequency pulse is exactly  $\pi/2$  radians, but the shape is rectangular, with a duration of one bit period. This has the effect of shifting the phase of the carrier by exactly one-quarter rotation over a span of one bit (or one-half symbol). The constellation and phase trellis for this waveform are depicted in Figure 2. At any instant in time, the phase is either stationary, or is moving at a constant rate of one-quarter of the bit rate. Viewed this way, SOQPSK appears to be a hybrid of QPSK and MSK.

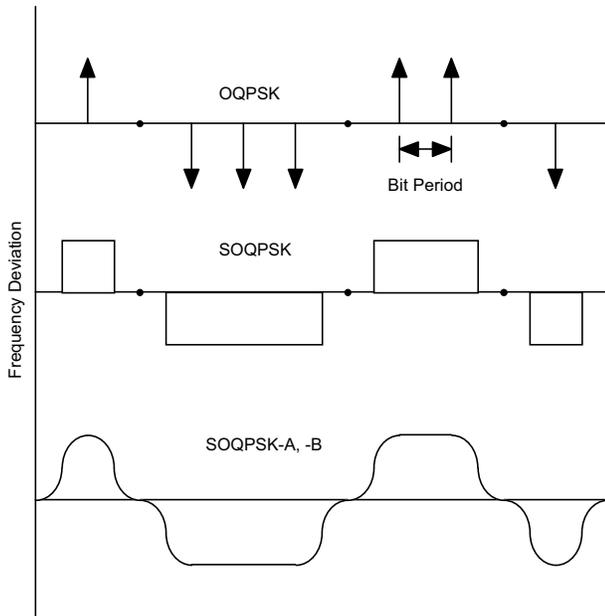


Figure 1. Frequency pulses for Offset QPSK variants.

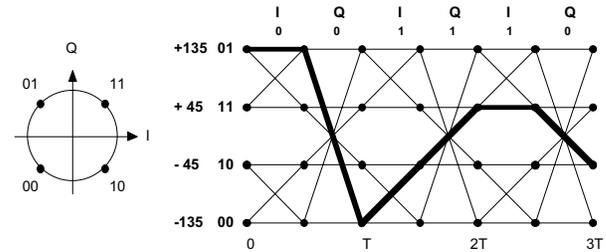


Figure 2. MIL-STD SOQPSK constellation

The bottom trace in Figure 1 represents the infinite family of other pulse shapes which will also shift the phase of the signal by  $\pi/2$  radians in one bit period. It's important to note that all of these waveforms are perfectly constant envelope (as expressed in Equation 1); only the phase trajectory differs from one variant to the next. It's also significant that all of these variations of OQPSK can be demodulated with a conventional OQPSK demod.

## SIMULATION RESULTS

The frequency pulse shapes for two new variants of SOQPSK, which we call SOQPSK-A and SOQPSK-B, are essentially minor modifications of the impulse response for the familiar spectral raised cosine filter. The mathematical definition of the SOQPSK-A and SOQPSK-B shapes,  $g(t)$ , are given by  $g(t) = n(t) * w(t)$ , where

$$n(t) = \frac{A \cos(\pi \rho B t / T)}{1 - 4(\rho B t / T)^2} * \frac{\sin(\pi B t / T)}{(\pi B t / T)} \text{ and}$$

$$w(t) = \begin{cases} 1, & \text{for } |t/T| < T \\ \frac{1}{2} + \frac{1}{2} \cos \frac{\pi(|t/T| - T_1)}{T_2}, & \text{for } T_1 < |t/T| < T_1 + T_2 \\ 0, & \text{for } |t/T| > T_1 + T_2 \end{cases}$$

As expressed above,  $n(t)$  is the impulse response of a spectral raised cosine filter with a rolloff factor of  $\rho$ , and an additional time-scaling factor of  $B$  in the time argument. If used without windowing,  $n(t)$  would have infinite extent on the time axis, so we have applied a simple raised cosine window,  $w(t)$ , to limit the duration of the frequency pulse. As in the earlier expressions,  $T$  is the symbol period (equal to two bit periods, since OQPSK carries two bits per symbol). The overall scaling factor  $A$  is used to normalize the pulse shape such that the phase shift induced by a single frequency pulse is  $\pi/2$  radians.

Note that the four parameters  $\rho$ ,  $B$ ,  $T_1$ , and  $T_2$  serve to completely define the frequency pulse shapes for SOQPSK-A and SOQPSK-B, as well as an infinite set of similar, and interoperable, waveforms. The specific values for SOQPSK-A and SOQPSK-B are tabulated below and the resulting pulse shapes are plotted in Figure 3.

Parameter	SOQPSK-A	SOQPSK-B
$\rho$	1.0	0.5
$B$	1.35	1.45
$T_1$	1.4	2.8
$T_2$	0.6	1.2

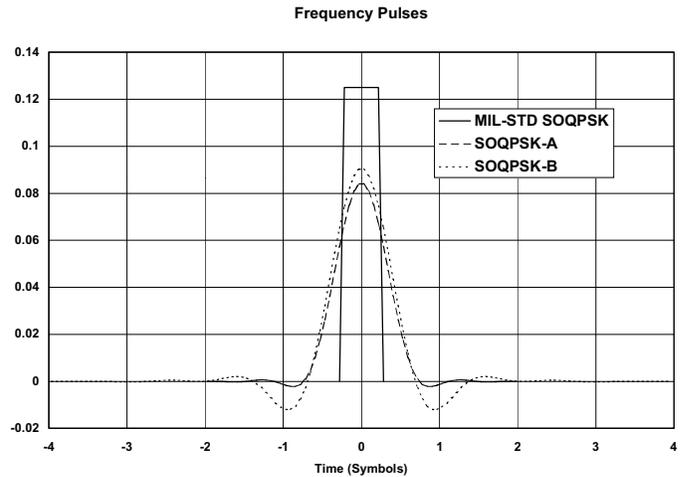


Figure 3. SOQPSK frequency pulse shapes.

The total duration of the frequency pulse, after application of the raised cosine window, is  $T_1 + T_2$ . This time span is four symbol periods for SOQPSK-B and only two periods for SOQPSK-A, so the  $-A$  version could be implemented in a lookup table only half the size of that needed for the  $-B$  version. In either case, however, the table size is quite modest.

The proposed values for  $\rho$ ,  $B$ ,  $T_1$ , and  $T_2$  are not “optimum” in any mathematical sense. Simulation results have shown that a relatively gradual tradeoff exists in these parameters; combinations which more tightly confine the spectrum tend to degrade BER performance slightly, and vice versa. The two cases here provide a representative example of what can be achieved within this functional form.

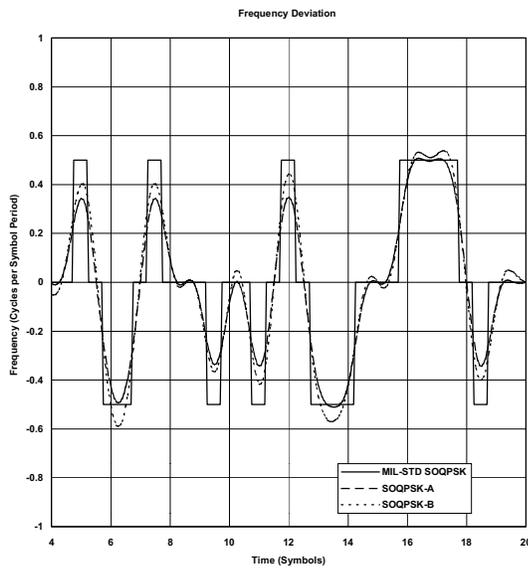


Figure 4. SOQPSK frequency deviation.

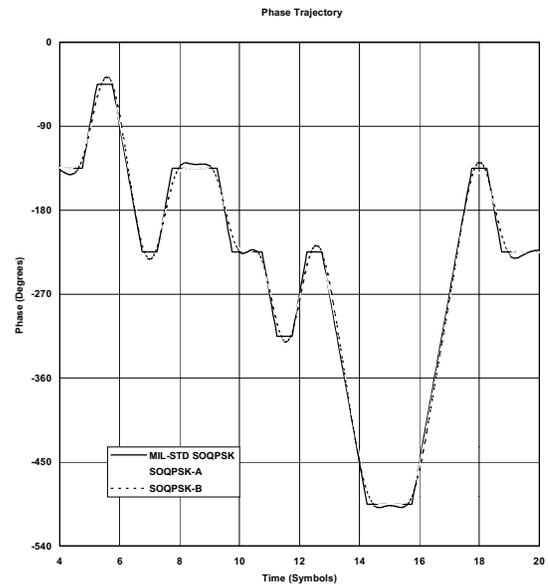


Figure 5. SOQPSK phase trajectories.

Figure 4 shows the instantaneous frequency deviation of MIL-STD SOQPSK, along with the  $-A$  and  $-B$  variations. Figure 5 depicts the corresponding phase trajectories. The close similarity of these waveforms leads to interoperability with each other, and with unshaped OQPSK as well.

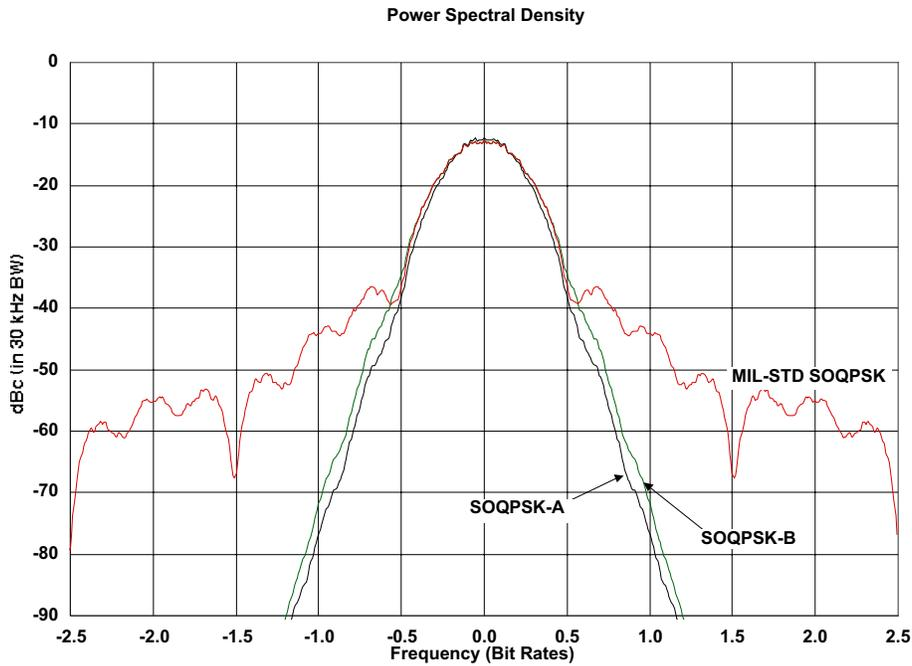


Figure 6. Simulated SOQPSK power spectral densities.

Figure 6 shows the simulated power spectral density for the three versions of SOQPSK. In this Figure, it becomes clear that changing the frequency pulse shape in the  $-A$  and  $-B$  versions has relatively little

effect on the spectrum down to nearly the  $-30$  dB point, but dramatically reduces the spectral sidelobes below that point.

The fact that the PSD of the MIL-STD version of SOQPSK is so much broader than the  $-A$  and  $-B$  versions at levels below about  $-30$  dB is an artifact of the initial application of the waveform. In the UHF SATCOM band for which SOQPSK was originally proposed and adopted, the link margin is typically only 10 dB or less, and interfering signals appear at relatively uniform levels (because the satellite is the common element in every link). Therefore, there was no significant advantage to controlling the spectrum at the lower levels; such levels are below the link noise floor. In terrestrial applications, however, interferers can be 60 to 70 dB above the desired signal (or more), so the superior spectral containment of the  $-A$  and  $-B$  versions is extremely important.

Figures 7 and 8 depict the eye pattern for the inphase channel of SOQPSK-A and  $-B$ , respectively. The quadrature channel for both waveforms is identical to the inphase component, except for a one-half symbol (one bit) time shift. Both of these eye patterns are captured directly out of the modulator; they do not reflect the effect of any IF or post detection filtering at the receiver.

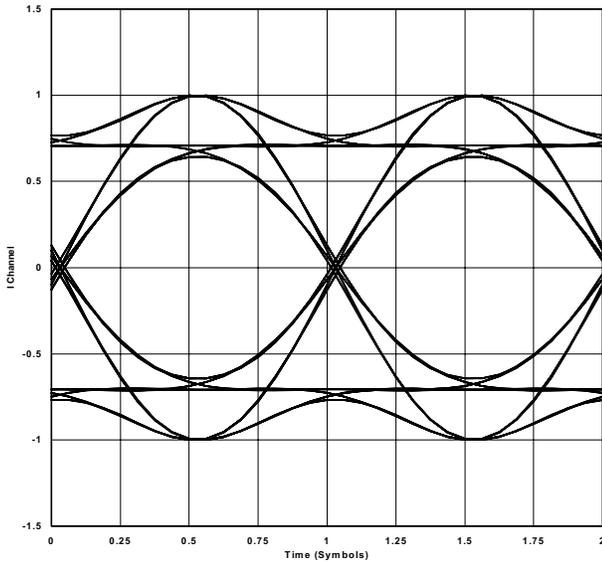


Figure 7. SOQPSK-A eye pattern.

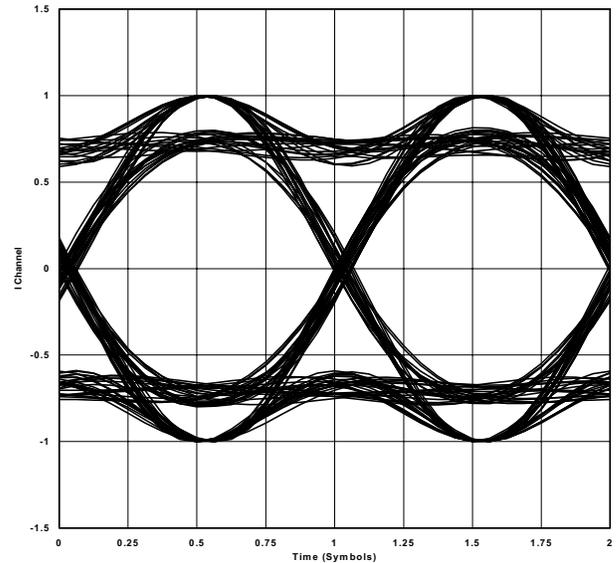


Figure 8. SOQPSK-B eye pattern.

The apparently greater intersymbol interference (ISI) in the  $-B$  eye pattern stems from the fact that the frequency shaping pulse (see Figure 3) is both longer and has larger peak-to-peak excursions than the pulse for the  $-A$  version. The net effect of the difference is that SOQPSK-A has a slightly narrower spectrum, but slightly poorer detection efficiency than SOQPSK-B (about 0.25 dB at BER =  $1e-5$ ).

## ARTM MEASURED RESULTS

The results presented above have been produced by computer simulation. To corroborate the simulation predictions with results from measured hardware, we used the facilities of the Advanced Range Telemetry (ARTM) Project at Edwards AFB. This facility was chosen because they have extensive

experience with Feher-patented FQPSK-B (Rev. A1), and they have a custom-built FQPSK-B (Rev. A1) demodulator, developed by RF Networks. This is significant because FQPSK-B (Rev. A1) offers performance comparable to SOQPSK-A and -B. Indeed, based on the results presented here, these three waveforms could be considered as alternatives to each other for many applications.

Figure 9 shows the PSD of FQPSK-B (Rev. A1) along with SOQPSK-A and -B. The results in this plot are taken directly out of the modulator, prior to the non-linear amplifier in the ARTM test fixture. Note that all three of the waveforms have nearly identical PSD characteristics down to about -25 dB. Below that level, FQPSK-B (Rev. A1) is the most compact, SOQPSK-A is slightly wider, and SOPQSK-B is wider still.

One of the key features of the SOQPSK variants being explored here is that the waveform is purely constant envelope; there is no AM component whatsoever. This is demonstrated in Figure 10, which shows the PSD of SOQPSK-A both before and after a nonlinear amplifier (NLA) stage. The spectrum is nearly identical on both sides of the NLA because there is no AM on the SOQPSK signal. Essentially identical results were measured for SOQPSK-B; the NLA had no effect on the spectrum.

Figure 11 presents this same comparison for FQPSK-B (Rev. A1), using the same NLA. The increase in occupied bandwidth for FQPSK-B (Rev. A1) is quite apparent. The author can only speculate on the cause of this effect, but a potential explanation is that FQPSK-B (Rev. A1) has some amplitude modulation component. If so, then this spectral broadening could be expected to vary from one amplifier to the next.

In order to compare SOQPSK-A with FQPSK-B (Rev. A1) under NLA conditions, the corresponding traces from Figures 10 and 11, are plotted together in Figure 12. Note that while FQPSK-B (Rev. A1) had a narrower spectrum than SOQPSK-A prior to the NLA, the reverse is true after the NLA.

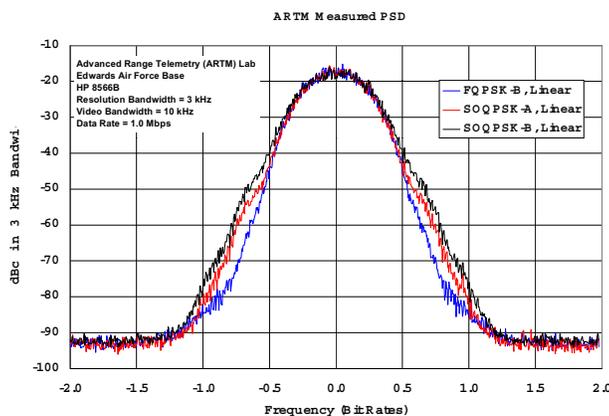


Figure 9. PSD, without nonlinear amplification.

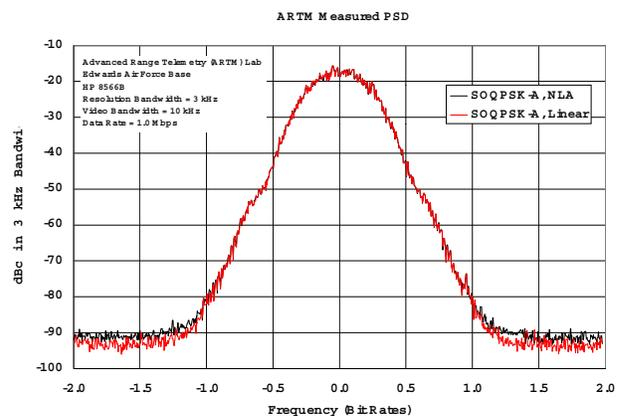


Figure 10. PSD for SOQPSK-A with and without nonlinear amplification.

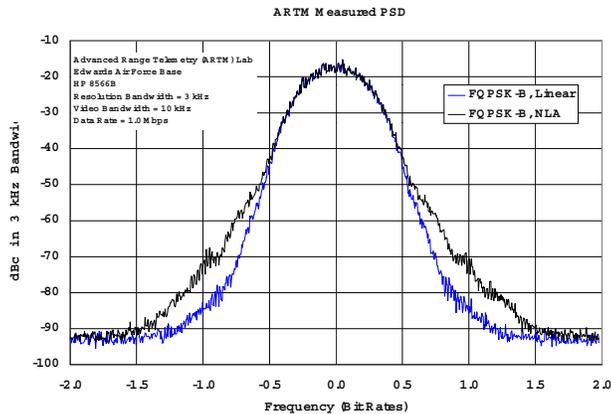


Figure 11. PSD for FQPSK-B (Rev. A1) with and without nonlinear amplification.

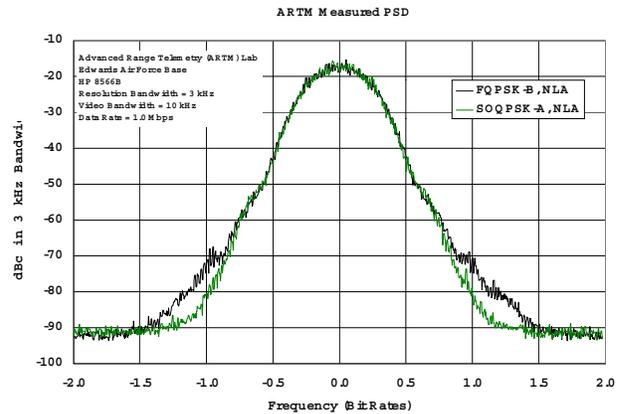


Figure 12. PSD of FQPSK-B (Rev. A1), and SOQPSK-A, nonlinearly amplified.

Of course, it's well known that the spectrum of a modulated signal can be bandlimited by a wide variety of methods; each approach exacts its own penalty in BER performance. The BER results presented in Figure 13 represent a comprehensive summary of the performance of SOQPSK-A, -B, and FQPSK-B (Rev. A1).

The three left-most BER curves in Figure 13 compare the performance of MIL-STD SOQPSK with SOQPSK-A and -B, using computer simulation. In the simulation, the demodulator is a completely conventional coherent offset QPSK demodulator; no differential encoding is used, and no special pulse shaping is employed to approximate matched filter detection of the shaped waveforms. It can be seen that this suboptimum detection strategy exacts a penalty of about 2.4 dB at BER =  $1e-5$  (relative to ideal OQPSK detection), but this penalty is essentially the same for all three variants of SOQPSK. It should be noted here that all of these versions of SOQPSK will in fact interoperate with each other, with only very small differences in BER performance (about 0.25 dB at BER =  $1e-5$ ). From this we conclude that existing MIL-STD SOQPSK modulators could be modified to generate SOQPSK-A or -B, with virtually no penalty in detection efficiency, but with considerable reduction in occupied bandwidth (in applications where the lower levels of the PSD are significant). It is worth noting here that matched filtering for SOQPSK is feasible, as is trellis demodulation. While the performance gains from these techniques are substantial, this is not addressed in the present paper.

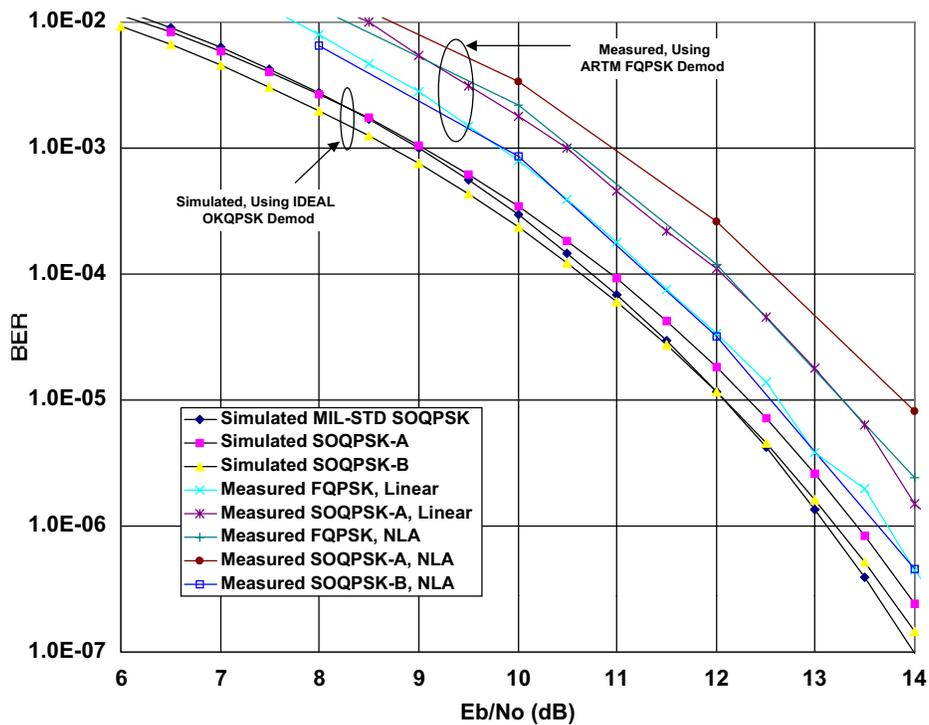


Figure 13. BER results for FQPSK-B (Rev. A1), MIL-STD SOQPSK, SOQPSK-A, and -B

The five right-most BER curves in Figure 13 are all taken using ARTM’s FQPSK-B (Rev. A1) demodulator, developed by RF Networks. This demodulator requires differential encoding of the signal to resolve the four-fold phase ambiguity inherent in these waveforms, which accounts for part of the difference in performance between the simulated and measured data. In the closely spaced measured curves (about 1.2 dB variation from best to worst), we find several interesting conclusions. The best performance is achieved by SOQPSK-B through the NLA, and FQPSK-B (Rev. A1) without the NLA. These two curves are virtually identical.

The distortion of the FQPSK-B (Rev. A1) signal which is incurred in passing through the NLA (exhibited as sidelobe regeneration in the PSD) also exacts a BER penalty of about 0.7 dB, relative to the un-amplified version.

Virtually overlapping the NLA curve for FQPSK-B (Rev. A1) is the curve for SOQPSK-A without the NLA. The right-most curve in the figure is for SOQPSK-A with the NLA. It is interesting to note that, although the NLA has virtually no effect on the PSD of the SOQPSK waveforms, the BER performance does exhibit about 0.5 dB degradation at  $BER = 1e-5$  due to the NLA. The author is not familiar with the design details of the RF Networks FQPSK-B (Rev. A1) demodulator, so any explanation of this effect would be highly speculative. We postulate that the FQPSK-B (Rev. A1) demodulator was able to efficiently recover the data from the SOQPSK-A and -B waveforms because all of these modulations are derivatives of offset QPSK.

## CONCLUSIONS

The results presented here answer several questions concerning constant envelope (or near constant envelope) versions of offset QPSK. First, we have provided a parametric description of a family of bandlimited, constant envelope OQPSK waveforms. Two members of this family have been analyzed in detail, and shown to provide BER and spectral characteristics which compare favorably with Feher-patented FQPSK-B (Rev. A1). We have shown by simulation that the BER performance of the –A and –B versions are within a small fraction of a dB of the MIL-STD version, using an ordinary offset QPSK demodulator.

In addition, we have shown via measured results from the ARTM lab that the members of the SOQPSK family interoperate with FQPSK-B (Rev. A1) in the sense that SOQPSK-A and SOQPSK-B have been correctly demodulated with a custom FQPSK-B (Rev. A1) demodulator. When operated through a non-linear amplifier, the BER performance of the SOQPSK-B is about 0.7 dB better than FQPSK-B (Rev. A1), which in turn, is about 0.5 dB better than SOQPSK-A.

These results suggest that the SOQPSK variants described here are viable alternatives to each other, as well as to FQPSK-B (Rev. A1), in applications where superior spectral containment is required, but detection efficiency cannot be compromised.

## ACKNOWLEDGEMENTS

The author would like to acknowledge the support of Mr. Robert Jefferis and Mr. Chuck Irving of the Advanced Range Telemetry (ARTM) Project at Edwards AFB, CA. They, and the other members of the ARTM team, have graciously provided the measured PSD and BER results in Figures 9 through 13, using their FQPSK-B (Rev. A1) demodulator for the BER results.